Modeling Flow of Magnetorheological Fluid through a Micro-channel

Nick M. Bruno*[1], Constantin Ciocanel[1], Allison Kipple[2]
[1]Dept. of Mechanical Engineering, Northern Arizona University
[2]Dept. of Electrical Engineering and Computer Sciences, Northern Arizona University
*Corresponding author: 240 West Saunders #139, Flagstaff, AZ 86001, nmb35@nau.edu

Abstract: This paper presents the approach taken through the utilization of COMSOL Multiphysics 3.5a, to develop a model that simulates the flow of a magnetorheological (MR) fluid through a micro-channel. The model was developed as an aid in the analysis of a micropump that produces flow by means of displacement of a MR fluid slug within a microchannel. The MR fluid slug is moved along the microchannel by a magnetic force that is generated by passing an electric current through a set of solenoids discretely located along the channel. Different pump layouts and magnetic circuit configurations were analyzed to maximize the magnetic field/force along the centerline of the micro-channel while minimizing the power required for the operation of the pump.

Keywords: MEMS, Magnetorheological Fluid, Micropump

1. Introduction

Most mechanical micropumps use a membrane to produce the pumping action; while a membrane can be actuated using several means and can be used to pump any kind of liquid, it has the disadvantage of producing a pulsed flow rather than a continuous one. Non-mechanical micropumps, like the MR fluid based pump analyzed here, have no moving parts and can generate continuous flows at different flow rates. MR fluids are suspensions of iron particles with diameters ranging from 5-15 μm. The carrier fluid may be water, oil or other liquids pending on the desired properties of the suspension specific to the application. In the presence of a moderate magnetic field, an MR fluid changes from a liquid to a solid-like state.

A MR fluid micropump produces flow by means of displacement of a MR fluid slug within a microchannel. The MR fluid slug is moved along the microchannel by a magnetic force that is generated by passing an electric current through a set of solenoids discretely located along the channel. While the MR fluid slug interacts directly with the pumped fluid, the immiscibility of the two fluids insures that the contamination of the later is avoided.

The MR fluid micropump produces a continuous flow and has low voltage requirements allowing for multiple, independently controlled pumps to be integrated on a single structure, thus enabling the development of complex microfluidic systems. This paper presents the model of a silicon dioxide (SiO_2) microchannel with solenoids discretely placed along its walls. By passing an electric current through the solenoids, a magnetic field gradient is generated across the microchannel; this field gradient creates a body force on the MR fluid slug which is transferred to the pumped fluid.

2. Theoretical considerations

The theory supporting the proposed pump is described below.

2.1 Magnetostatics

According to the Maxwell-Ampere law:

$$\nabla \times \overline{H} = \overline{J} \qquad (1)$$

where
$\overline{J}$ is the current density (A/m^2), and
$\overline{H}$ is the magnetic field (A/m).

To model a magnetic "pulse" along the microchannel, the external current density within each solenoid was modeled using the equation

$$J_{z1}^{e} = cdens \cdot \left(0.5 \cdot \cos\left(\omega t - shift\right) + 0.5\right) \qquad (2)$$

where
$cdens$ is the current density amplitude (A/m^2)
$\omega = 2\pi f$ is the traveling frequency (rad/s), and
$shift$ is the phase shift for each solenoid (rad).

The electromagnets placed along the channel can be supplied with a current density, defined by Equation (2), to generate a traveling magnetic wave throughout the channel. To achieve this,

the amplitude of the current density is varied from zero to *cdens* over a defined time interval.

In addition, Gauss's law assumes the nonexistence of magnetic monopoles [3], which translates into:

$$\nabla \cdot \overline{B} = 0 \tag{3}$$

Assuming that the electric field is constant and magnetic vector potential is $\overline{A}$, then

$$\nabla \times \overline{A} = \overline{B} \text{ and } \nabla \cdot \overline{A} = 0 \tag{4}$$

Since the simulation is run in 2D, it is assumed that the magnetic vector potential has only one nonzero value in the direction perpendicular to the working plane, i.e. $\overline{A} = (0,0,A_z)$.

Additionally, the magnetic and relative magnetic permeability of the micropump components were calculated as:

$$\mu = \mu_0(1-\chi) \tag{5}$$

$$\mu_r = \mu / \mu_0 \tag{6}$$

and

$$\chi = \mu_r - 1 \tag{7}$$

where

χ = magnetic susceptibility

μ = magnetic permeability [H/m]

μ_r = relative magnetic permeability

μ_0 = permeability of free space = $4\pi \cdot 10^{-7}$ [H/m].

Assuming that the MR fluid has a negligible hysteresis curve [2], the possible remnant flux densities are neglected throughout the simulation.

2.2 Flow Equations

The incompressible Navier-Stokes equations describe fluid flow within the microchannel as follows:

$$\rho \frac{\partial \overline{u}}{\partial t} - \nabla \cdot \eta\left(\nabla \overline{u} + (\nabla \overline{u})^T\right) + \rho \overline{u} \cdot \nabla \overline{u} + \nabla p = \overline{F}$$

$$\nabla \cdot \overline{u} = 0 \tag{8}$$

where

ρ is the fluid density (kg/m^3)

$\overline{u}$ is the velocity (m/s)

η is the fluid viscosity (Pa*s)

p is the pressure (Pa), and

$\overline{F}$ is the body force (N/m^3).

The body force in this simulation is derived from the divergence of the magnetic stress tensor [1], leading to the Kelvin force density

$$\overline{F} = \mu_0 \overline{M} \nabla \overline{H} \tag{9}$$

where

$\overline{M}$ is the magnetization (A/m), and

$\overline{H}$ is the magnetic field strength (A/m).

For the linear portions of the MR fluid magnetization curve [4]

$$\overline{M}(M_x, M_y) = \left(\frac{\chi \partial A_z}{\mu_0 \partial y}, \frac{-\chi \partial A_z}{\mu_0 \partial x} \right) \tag{10}$$

Substituting Equation (10) into (9) yields the force on an isolated body

$$F_x = \left(\frac{\partial A_z}{\partial x} \cdot \frac{\partial^2 A_z}{\partial x^2} + \frac{\partial A_z}{\partial y} \cdot \frac{\partial^2 A_z}{\partial x \partial y} \right) \cdot \left(\frac{\chi}{\mu_0 (1+\chi)^2} \right) \tag{11}$$

This force expression, together with Newton's Second Law, allows the calculation of the velocity of the MR fluid plug as follows:

$$F_x = m\overline{a} = m\frac{d\overline{u}}{dt} \Rightarrow \frac{d\overline{u}}{dt} = \frac{F_x}{m} \tag{12}$$

The velocity expression is included in the global equations and used by the ALE moving mesh application in COMSOL to describe the moving boundaries of the MR plug.

To this end, the simulation neglects viscous losses assuming a frictionless open ended microchannel.

3. Pump Configurations

During the course of this study, three configurations of the electromagnets along the microchannel have been simulated to identify the arrangement that yields the highest magnetic field inside the channel for a constant electric current density. In all the simulations, the MR fluid is initially located toward the left end of the microchannel which is surrounded by the pumped fluid to the left and right. As mentioned earlier, upon successive activation, the magnets induce a Kelvin force on the MR slug which in turn displaces the slug and the pumped fluid along the microchannel.

Figure 1 shows the three pump configurations that were considered in this study. In the first design, Figure 1.a., the three

solenoids surrounding a portion of the channel are assumed to have the same size as the MR fluid slug and to be separated just by a very thin insulation. In addition, the first solenoid (the one to the left) and the MR fluid slug were assumed to be at the same location along the channel, as it is shown in Figure 1.a.

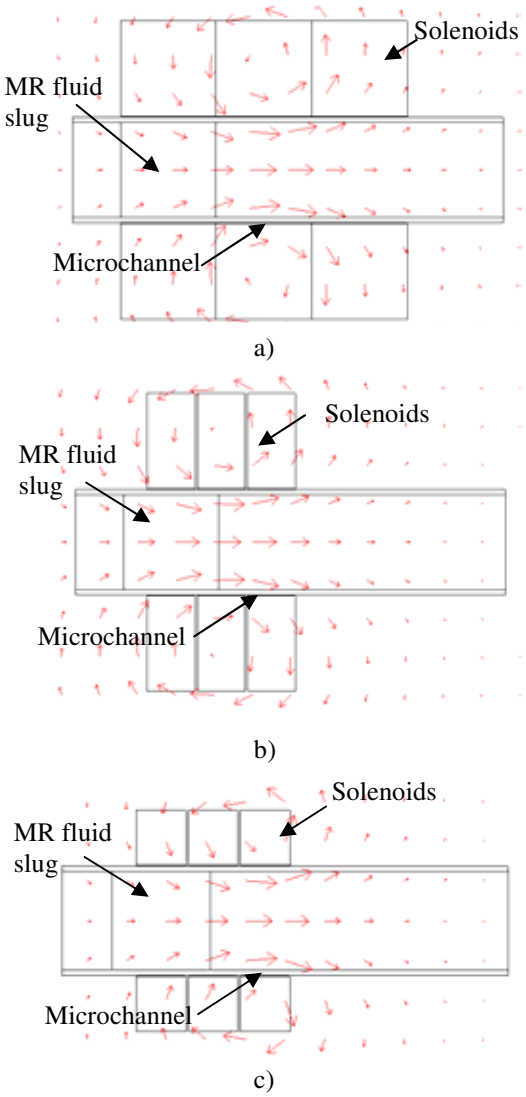

Figure 1: The three solenoid configurations analyzed.

In Figure 1, the red arrows indicate the magnetic field orientation, highlighting the flux lines are aligned with the direction of the flow inside the channel. By activating the solenoids successively, the MR fluid slug is dragged along the channel, pushing the pumped fluid along.

In the second configuration, Figure 1.b, the solenoid area was reduced by one half; a spacing of five micrometers was introduced between the solenoids and a spacing of two micrometers was introduced between the solenoids and the microchannel. In addition, the symmetry axis of the MR slug was not perfectly aligned with the symmetry axis of the first solenoid, causing an oscillating displacement to occur in the fluid before the slug reached force equilibrium. These changes in geometry, which translate into a reduction in length between the centers of the solenoids, allow for higher controllability of the MR slug and permit a faster traveling frequency, as discussed in Equation (2).

The third solenoid configuration, shown in Figure 1.c, was considered to evaluate the effect of further minimizing the coil cross sectional area on the overall field distribution across the channel. Accordingly, the solenoid height considered in Figure 1.b was cut in half, while preserving the spacing between solenoids and between solenoids and the channel. This change was expected to cause larger magnetic fields along the centerline of the microchannel with the coil center closer to the microchannel centerline. This configuration provides the same level of controllability as configuration two.

4. Design constraints

The target flow rate for the micropump was 6μL/min. This flow rate can be achieved with low field gradients if the inner diameter of the microchannel is small. In the current configuration, the inner channel diameter was 200 μm. To meet the desired flow rate, the MR slug needed to travel along the microchannel at a speed of 3.183 mm/s.

As the solenoids were assumed to be made of copper, to avoid their thermal degradation, the maximum current supplied to them was limited to 0.5 A.

Finally, the relative permeability for the MR fluid was assumed to be constant, with a magnitude of 4000; this is similar to that of iron.

5. Results

Using COMSOL's output data, the velocity of the plug was calculated as detailed below. After defining all preliminary variables, simulations were performed combining the Navier-Stokes, Magnetostatics, and ALE moving mesh modules in one analysis. Results showed displacement of the plug and development of boundary layer within the pumped fluid. Using the displacement from the plug boundaries and the simulation run time, the velocity was calculated for varying frequencies. The velocity was calculated using this method due to the mesh inversion occurring along the plug boundary. To avoid the mesh inversion, a script may be produced in Matlab and may be used to run the simulation in a loop. When using the Matlab script, a mesh quality stop condition should be added to the simulation to define where the simulation will stop to collect results and produce a new mesh from the deformed geometry. The simulation will then repeat, starting at the last time step found in the previous simulation. Figure 2 illustrates the displacement produced by the ALE moving mesh on the MR slug, while Figure 3 shows the induced velocity profile in the pumped fluid.

5.1 Results for the first configuration

To begin collecting results, pump configuration one was modeled such that each solenoid was touching another. The lack of spacing between solenoids was imposed for flow control purposes; reducing the spacing between the coils produced a constant strength in the field as the wave traveled from solenoid to solenoid. Separating the solenoids resulted in an area of low field strength between solenoids producing a reduced force and a varying velocity of the plug. When modeling a magnetic maximum traveling along the tube at a rate of 200 μm/s, the theoretical flow rate was found to be 6.28*10-3 μL/s. Figure 4 displays results for the flow rate, while varying the current in the solenoids. Table 1, from the Appendix, summarizes the geometry and simulation parameters for this configuration.

By varying the currents from 0.5 A to 1 A, the flow rate and velocity increased significantly, though this increase still does not match the speed of the maximum traveling field.

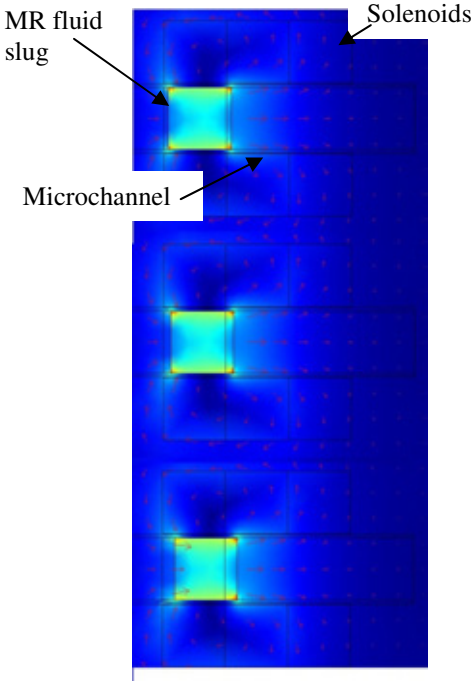

Figure 2: First solenoid's configuration – ALE moving mesh results.

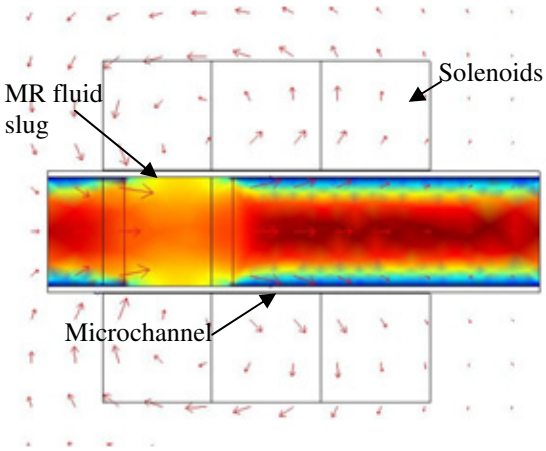

Figure 3: First solenoid's configuration – Induced velocity field in the pumped fluid.

In order to achieve the flow rate target value using a simple solenoid configuration, the currents had to be increased substantially to produce larger magnetic fields. However, at this scale, the solenoids would start to degrade even at low currents. It is safe to assume that implementing any current above 1 A is not plausible for this application. Figure 5 shows a comparison between the theoretical target flow

rate and the achievable flow rates with configuration one.

5.2 Results for the second configuration

To begin collecting results for configuration two, the pump was modeled such that the solenoids were reduced in size by one half along the vertical axis. The current input by Equation (2) produced a field similar to that found in Figure 1.b. It was found that by reducing the cross sectional area, the plug was more controllable and a reduction in current was permitted to provide the needed flow rates. Table 2 contains dimensions for simulations using configuration two and the results are shown in Figure 6.

Figure 6 shows that the MR plug can be moved with a frequency varying between 2 and 16 Hz with a current of 0.5 A. For this configuration to achieve the target flow rate of 6 μL/min, the needed wave frequency is 7.58 Hz. Figure 7 shows the flow rate readings for this configuration.

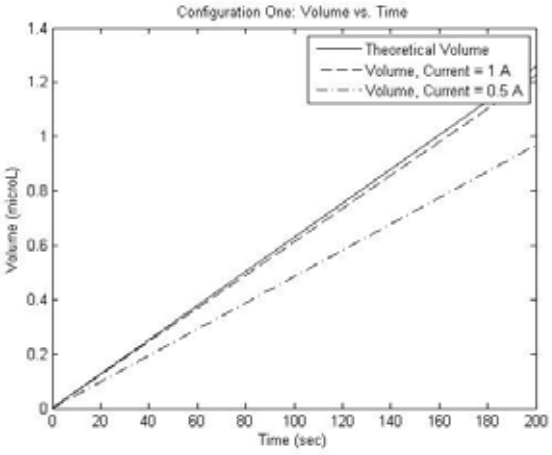

Figure 4: Configuration One – Volume vs. Time for varying currents.

As seen from Figure 7, approximately 0.1 μL/s can be pumped through the microchannel at 7.85 Hz. The modeled flow rate does not match the theoretical flow rate in various areas because of mesh quality and the velocity averaging.

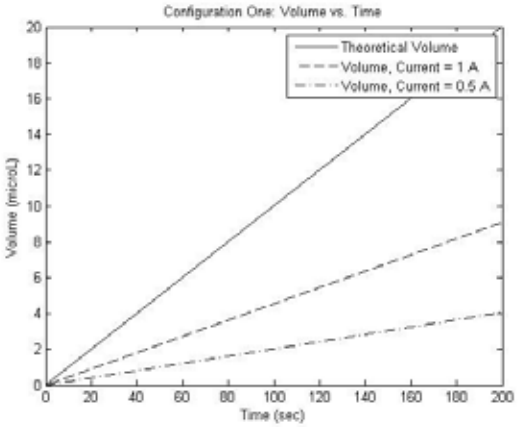

Figure 5: Configuration One – Comparison between target flow rate and achievable flow rates.

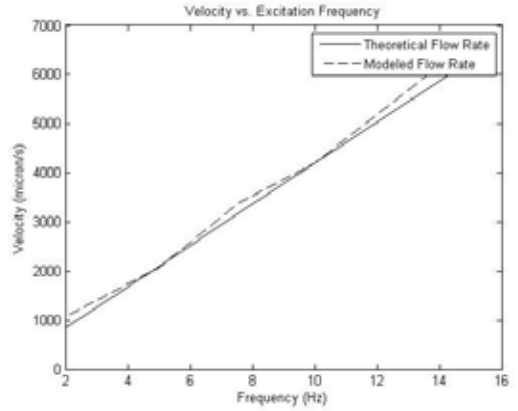

Figure 6: Configuration Two – Velocity vs. frequency at constant current = 0.5 A.

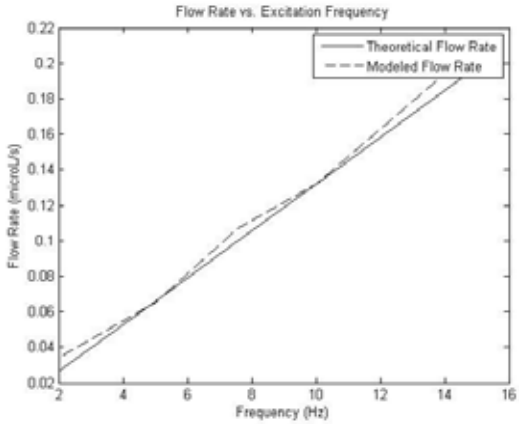

Figure 7: Configuration Two – Flow rate vs. frequency at constant current = 0.5 A.

In order to create flow in the micropump that was even more controllable, the electromagnets required more current to produce larger fields. However, this is not an option due to potential thermal degradation of the solenoids; configuration three was tested to see the effects of further reducing the size of the electromagnets which reduces the length between the coil centerline and the microchannel centerline.

5.1 Results for the third configuration

As stated above, configuration three was similar to that of configuration two. By reducing the solenoids to one half the size of those from configuration two, the magnetic field density increased on the microchannel centerline. Table 3 contains the geometry and simulation parameters for this configuration, while Figures 8 and 9 show the simulated velocity and flow rate, respectively.

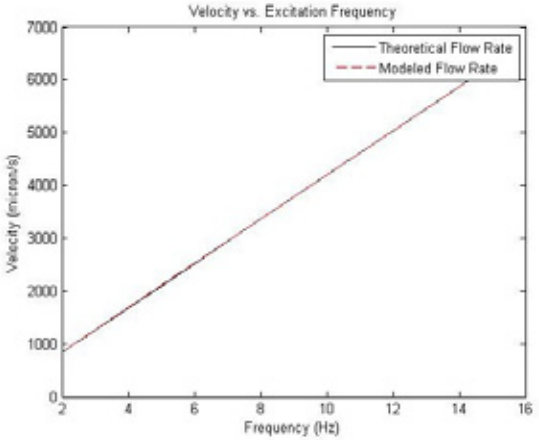

Figure 8: Configuration Three –Velocity vs. frequency.

It can be seen from the simulations that the difference between the theoretical and actual flow rates have been minimized by reducing the size of the coils. Ultimately, this was due to an increase in magnetic field produced by reducing coil size as by halving the height of the coil, the equivalent current moved closer to the channel. Again, the target flow rate was achievable with a frequency of 7.58 Hz which was dependent on the spacing between magnets and magnet size.

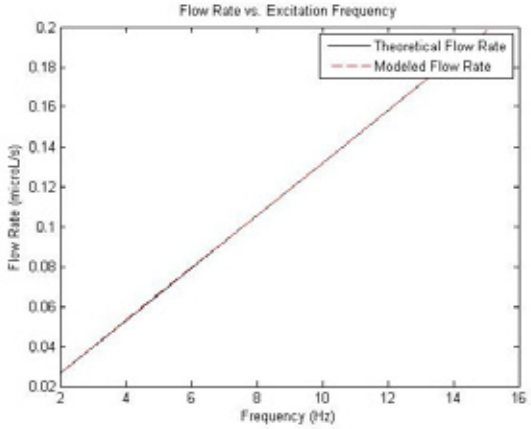

Figure 9: Configuration Three – Flow Rate vs. frequency.

6. Future Work

Future simulations will look into considering a variable frequency for transferring the magnetic maximum from one electromagnet to the next. This will facilitate the optimization of the pump by taking into account the momentum of the flow. In addition, an *m*-file will be created to run the simulation in a loop. This will produce more accurate results than the ones presented here, as the velocity averaging performed in this study will not be required. Future work may also entail consideration of ferrites in the design rather than the use of solenoids surrounding the microchannel; this will increase the available field strength near the channel, but due to the complexity of manufacturing micro-ferrites this option may not be fabricated in the future.

7. Conclusions

COMSOL Multiphysics was used to demonstrate that a fluid flow may be induced in a microchannel by moving an MR slug along the channel by means of a magnetic force. Curves for flow rate as a function of frequency were produced for three analyzed configurations. In these analyses, the current was kept constant at 0.5 A. The study showed that by selecting a proper configuration for the solenoids, a desired flow rate can be achieved. Upon reducing the size of the coils, larger magnetic gradients are seen along the centerline of the microchannel. Furthermore, not only can larger fields increase

the pumping velocities, but they also increase the controllability of the plug within the microchannel.

8. References

1. Rosensweig, *Ferrohydrodynamics*, 106-111. Cambridge, New York (1985)

2. Feynman, *The Feynman Lectures on Physics*, 34-1 to 36-15. Addison-Wesley, USA (1966)

3. Fleisch, *A Student's Guide to Maxwell's Equations*, 43-111. Cambridge, New York (2008)

4. Comsol Multiphysics, *Magnetic Drug Targeting in Cancer Therapy,* 2008

9. Acknowledgements

I would like to thank Dr. Constantin Ciocanel for the opportunity to work on this project and for his advice. I would like to thank Dr. Allison Kipple who has given me much guidance in magnetism topics.

10. Appendix

Table 1: Geometry and simulation parameters for the first solenoid's configuration

Current (A)	0.5	1.0
Frequency (Hz)	0.5	0.5
Shift (rad)	π	π
Coil Area (μm^2)	40 000	40 000
Coil Spacing (μm)	Touch	Touch
Coil Spacing from Wall (μm)	2	2
Max Field On Microchannel Centerline (mT)	0.84	1.7

Table 2: Geometry and simulation parameters for the second solenoid's configuration

Current (A)	0.5
Shift (rad)	π
Coil Area (μm^2)	20 000
Coil Spacing (μm)	5
Coil Spacing from Wall (μm)	2
Max Field On Microchannel Centerline (mT)	1.54

Table 3: Geometry and simulation parameters for the third solenoid's configuration

Current (A)	0.5
Shift (rad)	π
Coil Area (μm^2)	11 200
Coil Spacing (μm)	5
Coil Spacing from Wall (μm)	2
Max Field On Microchannel Centerline (mT)	1.80